



The excitation and propagation of elastic waves in multilayered anisotropic composites[☆]

Ye.V. Glushkov*, N.V. Glushkova, A.S. Krivonos

Krasnodar, Russia

ARTICLE INFO

Article history:
Received 27 April 2009

ABSTRACT

Using an integral approach wave fields, excited by dynamic action on composite materials with an arbitrary anisotropy of the elastic properties of their layers, are expressed in the form of the convolution of a Green's matrix with the stress vector of the specified load. The construction of a Fourier symbol of Green's matrix and the location of their poles and residues in them, which gives the asymptotic form of the surface and channel waves, plays a key role in determining the dynamic reaction of the material and in analysing the wave fields. Unlike the representations of classical modal analysis, the latter takes into account not only the characteristics of the material but also of the source. A brief description of the general scheme of wave analysis is given and test numerical examples are presented, as well as examples of the effect of the material structure on the energy characteristics and directivity of the radiation of waves excited in them by surface piezoactuators.

© 2010 Elsevier Ltd. All rights reserved.

Many composites are multilayer structures with, as a rule, sharply differing, anisotropic and mechanical properties of the components of their layers, which makes it extremely difficult to calculate both the stress-strain state and the dynamic behavior of articles made of these materials. Considerable computational difficulties also arise due to the complex structure of the wave fields, which are formed as a result of multiple rereflections of the waves at the layer boundaries.

The problems that arise here can be conventionally divided into the following groups:

- 1) *modal analysis*, i.e., the determination of the wave characteristics (the phase and group velocities, the natural oscillation modes, etc.), inherent in the sample considered, irrespective of the dependence on the applied load;
- 2) *ray analysis* of the transformation of the specified incident wave in the layered structure (reflections, refractions, etc.);
- 3) *determination of the dynamic response* to a specified force (contact) action;
- 4) *amplitude and energy analysis*, i.e., the determination of the amplitude characteristics of the waves excited by a specified load, the directivity of the radiation, the spatial structure of the energy fluxes, the characteristics of the reflected waves which arise as a result of diffraction at local inhomogeneities (defects), etc.

The technique of modal and ray analysis of anisotropic laminated waveguides is quite well developed. The methods and approaches used here,^{1,2} as a rule, go back to the Thomson–Haskell–Petraschen matrix algorithms proposed in the 1950s for a packet of isotropic elastic layers (see, for example, the review Ref. 3). In this approach, the construction of dispersion relations for normal modes is reduced to finding the zeros of the determinant of the matrix formed from the boundary conditions between the layers, while the natural forms of normal modes are expressed in terms of corresponding eigenvectors of this matrix.

The dynamic response of extended structural components is usually calculated using simplified theories, in which the dependence of the stress and strain fields on the transverse coordinates is assumed to be linear, as in the Kirchhoff–Love theory of plates, or quadratic or cubic, as in the higher-order theories.^{4,5} In cases when the wavelength becomes comparable with the plate thickness, for example, for high-frequency or shock excitation, the hypotheses which are the basis of approximate theories cease to work, and the need arises to carry out calculations in a complete three-dimensional formulation. At the present time finite element or finite difference packages are usually

[☆] Prikl. Mat. Mekh. Vol. 74, No. 3, pp. 419–432, 2010.

* Corresponding author.

E-mail address: evg@math.kubsu.ru (Ye.V. Glushkov).

employed for this purpose in engineering practice. However, in view of the natural limitations of the admissible number of elements of grid discretization, standard finite element and finite difference methods are only used for finite bodies or limited regions, adjoining the load region, and the actual dimensions achieved are smaller the more complex the structure of the material and the excited wave fields.

For this reason these methods, based on grid approximation, are not well adapted for solving problems of the fourth group, which arise, for example, when developing methods of ultrasonic flaw detection or remote wave monitoring of structures using a distributed system of piezoactuators and sensors (SHM - structural health monitoring^{6,7}). To overcome these limitations hybrid schemes have been developed in which the solutions, in the form of an expansion in normal modes, constructed by modal analysis methods, are matched on the boundary of the region of grid discretization with the numerical solutions obtained using the finite element or finite difference methods.⁸ In fact, in the package of the finite element method so-called “infinite elements” are introduced, which rigorously take into account the structure of the wave fields radiated from the source (the region of application of the load) at infinity.

This purpose is achieved in a more natural way using an integral approach, based on a representation of the wave field in the form of the convolution of Green’s matrix of the packet of layers or laminated half-space considered with its excitation by a surface load^{9–11} The reduction of the contour integrals, which occur in the representation of Green’s matrix, to the sum of residues gives the required expansion of the wave field in normal modes. Information on the source occurs in such an expansion automatically in terms of the specified load function, and hence no complex matching procedure with the numerical solution in the near zone is required here.

Note that problems of modal analysis are also solved using the integral approach: the poles of the Fourier symbol of Green’s matrix are wave numbers, while the residues in them are natural forms of normal modes. Integral representations are also used when solving problems of the third group. Displacements of the surface into the region of application of the load, that are necessary to analyse the dynamic response of the material, are determined by numerical integration, or (for specified displacements into the contact zone) the problem is reduced to an integral equation of the convolution type with respect to the unknown contact stresses.⁹

Below we describe the integral approach to solving problems of wave monitoring of composite materials, i.e., multilayer waveguides with an arbitrary anisotropy of the component layers.

1. The general wave analysis scheme

For laminar waveguides, the residues at real poles make the main contribution to the asymptotic form of the travelling waves. The corresponding mathematical technique has been repeatedly described, including in the educational literature, but, as a rule, using the example of isotropic media. Papers in which three-dimensional anisotropic waveguides are considered are much rarer, and hence below we will give a brief description of the derivation of the fundamental relations employed later for the numerical analysis.

A harmonic wave field $\mathbf{u}e^{-i\omega t}$, excited by a load $\mathbf{q}e^{-i\omega t}$, applied in a certain region Ω to the surface $z=0$ of an elastic waveguide with plane-parallel boundaries, can be represented in the form

$$\begin{aligned} \mathbf{u}(\mathbf{x}) &= \iint_{\Omega} k(x - \xi, y - \eta, z) \mathbf{q}(\xi, \eta) d\xi d\eta \equiv \\ &\equiv \frac{1}{(2\pi)^2} \iint_{\Gamma_1 \Gamma_2} K(\alpha_1, \alpha_2, z) \mathbf{Q}(\alpha_1, \alpha_2) e^{-i(\alpha_1 x + \alpha_2 y)} d\alpha_1 d\alpha_2 \end{aligned} \quad (1.1)$$

It is assumed that the medium occupies the volume $-\infty \leq x, y \leq \infty, -H \leq z \leq 0$; when $H = \infty$ this is an elastic stratified half-space, $\mathbf{x} = \{x, y, z\}$ is the vector of spatial coordinates, $K = \mathcal{F}[k]$ and Eq. (421d) are Fourier symbols (i.e., the result of a Fourier transformation \mathcal{F} with respect to the horizontal coordinates x and y) of the matrix function $k(\mathbf{x})$ and the vector function $\mathbf{q}(x, y)$, and Γ_1 and Γ_2 are the integration contours of the inverse Fourier transformation \mathcal{F}^{-1} , the deviation of which from the real axes $\text{Im}\alpha_m = 0 (m=1,2)$ is fixed in accordance with the limit-absorption principle. Here and henceforth we will use, as far as possible, the notation and ideas traditional for the previous papers.^{10–12}

In polar coordinates

$$\alpha_1 = \alpha \cos \gamma, \quad \alpha_2 = \alpha \sin \gamma, \quad x = r \cos \varphi, \quad y = r \sin \varphi, \quad z = z$$

$$r = \sqrt{x^2 + y^2}, \quad \alpha = \sqrt{\alpha_1^2 + \alpha_2^2}, \quad 0 \leq \varphi, \quad \gamma \leq 2\pi$$

representation (1.1) takes the form

$$\mathbf{u}(\mathbf{x}) = \frac{1}{(2\pi)^2} \int_0^{2\pi} \int_{\Gamma} K(\alpha, \gamma, z) \mathbf{Q}(\alpha, \gamma) e^{-i\alpha r \cos(\gamma - \varphi)} \alpha d\alpha d\gamma \quad (1.2)$$

Here Γ is the contour which goes along the positive real semiaxis $[0, \infty]$, deviating from it when going round the real poles $\zeta_n (n=1, \dots, N)$, as a rule, in the lower half-plane $\text{Im}\alpha < 0$ of the complex plane α . Only so-called irregular poles with a negative angle of inclination of the tangent $d\zeta_n/d\omega$ are circumvented from above.⁹

Representation (1.2) holds both for isotropic and anisotropic waveguides, and not only for homogeneous but also for multilayer waveguides with an arbitrary piecewise-continuous dependence of the elastic properties on the vertical coordinate z (functionally graded media). The only difference is the specific form and properties of the matrix K . For isotropic media the dependence of its elements on the angular coordinate γ in the representation $k(r, \phi, z)$ reduces to Bessel functions Eq. (4211) from Russian, while the remaining single integral over α when $H < \infty$ can be exactly replaced by a series in residues at the poles ζ_n , which describe cylindrical waves, expressed in terms of Hankel

functions $H_m^{(1)}(\zeta_n r)$. Anisotropy of the elastic properties leads to a dependence of K on γ which, in general, does not enable us to obtain an explicit analytical representation of the integrals over γ and correspondingly explicitly calculate $k(\mathbf{x})$ in the form of a series in residues. Hence, here we will derive the asymptotic forms of the surface and channel waves using a different scheme.

For $r > r_0$, where r_0 is the radius of the circle which wholly contains the region Ω of decrease or increase in the integrand (1.2) in the complex plane, α depends only on the sign of the exponent. By Jordan's lemma the contour Γ can close in the upper half-plane for γ such that $\cos(\gamma - \varphi) \leq 0$ and, correspondingly, in the lower half-plane for the remaining ones. Further, using Cauchy's theorem on residues and estimating the behaviour of the integrals along the closing imaginary semi-axes $[i\infty, 0]$ and $[-i\infty, 0]$, and also on the edges of the cuts (in the case of a half-space $H = \infty$) as $O((r\kappa)^{-3/2})$, $r\kappa \rightarrow \infty$, we arrive at the representation

$$\begin{aligned} \mathbf{u}(\mathbf{x}) &= \sum_{n=1}^N \mathbf{u}_n(r, \varphi, z) + O((r\kappa)^{-3/2}), \quad r\kappa \rightarrow \infty \\ \mathbf{u}_n &= \frac{i}{2\pi} \int_0^\pi \mathbf{b}_n(\theta, z) e^{i\zeta_n(\theta)r \sin\gamma} d\gamma, \quad \theta = \gamma + \varphi + \pi/2 \\ \mathbf{b}_n(\gamma, z) &= j_n \operatorname{res}[K(\alpha, \gamma, z) \mathbf{Q}(\alpha, \gamma) \alpha] |_{\alpha = \zeta_n(\gamma)} \end{aligned} \quad (1.3)$$

$\kappa = \omega/v$ is the wave number corresponding to the characteristic velocity of propagation of the waves v , $j_n = 1$ for regular ζ_n and $j_n = -1$ for irregular ζ_n . The vector functions \mathbf{u}_n are normal modes, excited in the composite material by the load \mathbf{q} . In the far zone $r\kappa \gg 1$ the main contribution to the asymptotic representation is made by the stationary points γ_m of the phase function $s_n(\gamma) = \zeta_n(\theta) \sin\gamma$ of integral (1.3) (Ref. 13)

$$\begin{aligned} \mathbf{u}_n(r, \varphi, z) &\sim \sum_m \mathbf{d}_{n,m}(\varphi, z) e^{is_n(\gamma_m)r} / \sqrt{r}; \quad \mathbf{d}_{n,m} = \mathbf{b}_n(\theta_m, z) / \sqrt{2\pi is_n''(\gamma_m)} \\ \gamma_m: s_n'(\gamma_m) &= 0, \quad \theta_m = \gamma_m + \varphi + \pi/2 \end{aligned} \quad (1.4)$$

In the isotropic case the poles ζ_n are independent of γ , and in the section $[0, \pi]$ there is a single stationary point $\gamma_1 = \pi/2$, which is independent of the direction of the radiation of the waves ϕ considered. In the anisotropic case, the equation for determining the stationary points reduces to the form $\operatorname{ctg}\gamma = -\zeta_n'(\theta)/\zeta_n(\theta)$, i.e., the roots γ_m are points of intersection of the curve $-(\ln\zeta(\theta))'$ with the graph of the cotangent.

Representation (1.4) is convenient both for modal and for amplitude analysis. Its terms describe cylindrical waves propagating from the source, which attenuate with distance as $(r\kappa)^{-1/2}$. These are Rayleigh–Lamb, Stoneley and Love waves, the wave numbers of which $s_n(\gamma_m)$ (and, correspondingly, the phase and group velocities $v_n = \omega/s_n$ and $c_n = d\omega/ds_n$) depend on the direction of the radiation ϕ . The amplitude factors $\mathbf{d}_{n,m}$, which determine the energy and directivity of the radiation, depend both on the structure of the material, information on which is taken into account in the elements of the matrix K , and also on the source, the effect of which on the characteristics of the excited field occur via the vectors $\mathbf{Q}(\zeta_n, \gamma_m)$.

This representation becomes an effective instrument for rapid parametric analysis only if a reliable algorithm is available for constructing the matrix K , searching for the poles ζ_n and calculating the residues $\operatorname{res} K|_{\alpha = \zeta_n}$.

2. An algorithm for constructing Green's matrix

For homogeneous elastic media (a half-space or layer) the elements of the matrix K can be obtained in explicit form, not only for isotropic media but also for certain classes of anisotropy, for example, for an orthotropic material.¹⁴ However, for multilayered and all the more for graded media, as a rule, it is not possible to write the matrix K in explicit form. (Theoretically, using symbol-computational packages, such as MATHEMATICA or MAPLE, one can also obtain analytical representations in the case of a piecewise-constant dependence on the depth, but in view of their extreme length they are not very useful in practice.) Hence, in the 1970s–1980s numerical-analytical methods of constructing the matrix K were intensively developed to use the integral approach to such media. The main complexity when using these methods in practice is connected with the exponential dependence of the components of the solution on the z coordinate, which leads to numerical instability.

The algorithm described below is a generalization to the anisotropic case of the approach in Refs 10 and 12, developed for isotropic multilayered and graded media, in which numerical stability is ensured by a special removal of the “poor” exponential components out of the numerical procedures. A numerical-analytical approach was then developed to constructing the matrix K for homogeneous media with arbitrary anisotropy,¹ realized in application to modeling surface acoustic waves in piezoelectric crystals,² but it was not described in detail.

Suppose, to be specific, as previously,¹² we consider an M -layered composite material of thickness H with outer faces $z=0$ and $z=-H$ free from stresses $\tau = \{\tau_{xz}, \tau_{yz}, \tau_z\}$ (with the exception of the region where the load q is applied):

$$\tau|_{z=0} = \mathbf{q}, \quad \tau|_{z=-H} = \mathbf{0}; \quad \mathbf{q}(x, y) \equiv \mathbf{0} \text{ при } (x, y) \notin \Omega \quad (2.1)$$

¹ Glushkov YeV, Syromyatnikov PV, Analysis of wave fields excited by a harmonic surface source in an anisotropic half-space. Krasnodar, 1985. Manuscript presented at the Kuban State University. Deposited at VINITI 7 August 1985, No. 5861–85.

² Syromyatnikov PV. The energy of electroelastic waves excited by a harmonic surface source in a semibounded piezoelectric medium. Candidate Dissertation 1 February 2004, Kuban State University, 1996.

On the internal boundaries $z = z_k$ which constitute its anisotropic layers

$$D_k: -\infty < x, y < \infty, \quad z_{k+1} \leq z \leq z_k \quad (z_1 = 0, \quad z_{M+1} = -H)$$

the following rigid coupling conditions are specified

$$[\mathbf{u}]_k = 0, \quad [\boldsymbol{\tau}]_k = 0, \quad k = 2, 3, \dots, M \quad (2.2)$$

where $[\mathbf{f}]_k = \lim_{z \rightarrow z_k^-} \mathbf{f} - \lim_{z \rightarrow z_k^+} \mathbf{f}$ is the jump in the corresponding vector function. Modification of the algorithm given below for other boundary conditions is fairly simple.

In view of the arbitrary anisotropy of the layers it will henceforth be more convenient to use tensor notation with numerical indexation of the coordinates ($\mathbf{x} = \{x_1, x_2, x_3\}$ etc.) and summation over like indices. The equations of motion, Hooke's law and the Cauchy relations in each of the layers D_k have the form

$$\sigma_{ij,j} + \rho \omega^2 u_i = 0, \quad \sigma_{ij} = C_{ijkl} \varepsilon_{kl}, \quad \varepsilon_{kl} = (u_{k,l} + u_{l,k})/2; \quad i, j = 1, 2, 3 \quad (2.3)$$

Here σ_{ij} and ε_{ij} are the components of the stress and strain tensors, C_{ijkl} are the components of the elasticity constants tensor and ρ is the density; we will denote by a comma in the subscript, as is usually done, a derivative with respect to the corresponding spatial coordinate: $u_{ij} \equiv \partial u_i / \partial x_j$ etc. It is assumed that C_{ijkl} and ρ are piecewise-constant functions of the depth $z \equiv x_3$, which take constant values within each layer D_k .

By substituting the stresses σ_{ij} , expressed in terms of the strains u_i , into the equations of motion (2.3), we reduce them to the equations of elastodynamics

$$C_{ijkl} u_{l,jk} + \rho \omega^2 u_i = 0, \quad i = 1, 2, 3 \quad (2.4)$$

In the isotropic case we apply a Fourier transformation with respect to the horizontal coordinates x, y to these equations, which degenerate into the well-known Lamé equations, and construct fundamental solutions of the system of ordinary differential equations in z , obtained as a result. Here, however, these calculations impair the compactness of the tensor notation. This compactness can be preserved if we formally apply a Fourier transformation $\mathcal{F}_{\mathbf{x}}$ over all three spatial coordinates and, taking into account the property of the transformation of derivatives

$$\mathcal{F}_{\mathbf{x}} \left[\frac{\partial^2 u}{\partial x_j^2} \right] = (-i\alpha_j)^n U(\boldsymbol{\alpha})$$

consider the factor $(-i\alpha_3)^n$ which appears as an operator form of the derivatives d^n/dz^n .

As a result, for each of the layers D_k , Eqs (2.4) is reduced to a homogeneous system of ordinary differential equations in the Fourier transformation of the displacements $\mathbf{U}(\alpha_1, \alpha_2, z) = \mathcal{F}_{xy}[\mathbf{U}]$:

$$[B(\boldsymbol{\alpha}) - \rho \omega^2 I] \mathbf{U} = 0; \quad \boldsymbol{\alpha} = (\alpha_1, \alpha_2, \alpha_3) \quad (2.5)$$

Here I is the identity matrix, while the matrix components $B = \|b_{ij}\|$, which are the matrix form of the notation of the Christoffel tensor of an anisotropic elastic medium,⁵⁻¹⁵ have the form $b_{ij} = C_{ijkl} \alpha_k \alpha_l$. When the characteristic equation of system (2.5)

$$\det[B(\boldsymbol{\alpha}) - \rho \omega^2 I] = 0 \quad (2.6)$$

considered with respect to the characteristic numbers, has no multiple roots $\lambda_n = -i\alpha_{3,n}(\alpha_1, \alpha_2, \omega)$, or, when there are multiple roots, only linearly independent eigenvectors \mathbf{m}_n correspond to them (i.e., the Jordan form is diagonal, and there are no associated vectors in the Jordan basis), its general solution can be written in the form

$$\mathbf{U}(\alpha_1, \alpha_2, z) = \sum_{n=1}^6 t^{(n)} \mathbf{m}_n e^{\lambda_n z}$$

$$\mathbf{m}_n: [B(\boldsymbol{\alpha}_n) - \rho \omega^2 I] \mathbf{m}_n = 0, \quad \boldsymbol{\alpha}_n = (\alpha_1, \alpha_2, \alpha_{3,n}(\alpha_1, \alpha_2, \omega)) \quad (2.7)$$

where $t^{(n)}$ are arbitrary constants. Summation is carried out here up to $n=6$, since the characteristic equation (2.5) is a sixth-degree polynomial in α_3 .

Fortunately, the set of values of the input parameters α_1, α_2 and ω , for which Jordan blocks occur, and the form (2.7) becomes unusable, has measure zero, and hence this block is numerically unstable, breaking down with minimum change of one of the parameters.³ A unique important special case, when there are multiple roots for all α_1 and α_2 , and the general solution is expressed not only in terms of eigenvectors but also in terms of associated vectors, is when $\omega=0$, i.e., statics.

In the isotropic case there is a pair of single roots $\pm\sigma_1$ and a pair of double roots $\pm\sigma_2$ of λ_n , which are written in explicit form: $\sigma_j = \sqrt{\alpha^2 - \kappa_j^2}$, where $\kappa_j = \omega/v_j$ ($j=1, 2$) are the wave numbers of bulk longitudinal and transverse waves. The degenerate case, for which,

³ Nagornyi SV, Cherkasov IV. Location of the acoustic axes in crystals by reducing the Christoffel tensor to an upper Hessenberg form. Krasnodar, 1984. Manuscript presented at the Kuban State University. Deposited at VINITI 6 July 1984, No. 4763–84.

when $\omega > 0$, expansion (2.7) is inapplicable, only occurs at branching points κ_j , when $\sigma_j = 0$. However, it is not necessary to calculate the matrix K in them, since they are circumvented by the integration contour.

In the anisotropic case, the roots of Eq. (2.6) can also be split into two groups:

$$\lambda_j = \sigma_j, \quad \lambda_{j+3} = -\sigma_j, \quad j = 1, 2, 3$$

and by ordering them in a similar way:

$$\operatorname{Re}\sigma_1 \geq \operatorname{Re}\sigma_2 \geq \operatorname{Re}\sigma_3 \geq 0, \quad \operatorname{Im}\sigma_1 \leq \operatorname{Im}\sigma_2 \leq \operatorname{Im}\sigma_3 \leq 0$$

in the isotropic case they will be identical with the radicals given above (where $\sigma_3 \equiv \sigma_2$).

Fixing of the branches σ_j is important both to satisfy the conditions at infinity $z = -\infty$ in the case of a half-space, and to ensure numerical stability in the case of a multilayer package. In the first case, it is sufficient to retain the first three terms in representation (2.7), putting $t^{(4)} = t^{(5)} = t^{(6)} = 0$, and in the second, instead of representation (2.7), we propose to use the general solution in the following modified form:

$$\mathbf{U} \equiv \mathbf{U}_k = \sum_{j=1}^3 [t_k^{(j)} \mathbf{m}_j e^{\sigma_j(z-z_k)} + t_k^{(j+3)} \mathbf{m}_{j+3} e^{-\sigma_j(z-z_{k+1})}], \quad z \in D_k, \quad k = 1, 2, \dots, M \tag{2.8}$$

The unknown coefficients of the expansion $t_k^{(j)}$, grouped in the vector \mathbf{t} of length $6M$:

$$\mathbf{t} = \{t_1, t_2, \dots, t_M\}, \quad \mathbf{t}_M = \{t_k^{(1)}, t_k^{(2)}, \dots, t_k^{(6)}\}$$

are determined from the algebraic system

$$A\mathbf{t} = \mathbf{f} \tag{2.9}$$

which arises after substituting the general solution (2.8) into the Fourier transformed boundary conditions (2.1) and (2.2).

The external $6M \times 6M$ matrix A has the same partitioned structure as in the isotropic case (see, for example, Ref. 12, formula (3.3)):

$$A = \begin{pmatrix} S_1^+ & 0 & 0 & \dots & 0 & 0 \\ C_1^- & -C_2^+ & 0 & \dots & 0 & 0 \\ 0 & C_2^- & -C_3^+ & \dots & 0 & 0 \\ \dots & \dots & \dots & \dots & \dots & \dots \\ 0 & 0 & 0 & \dots & C_{M-1}^- & -C_M^+ \\ 0 & 0 & 0 & \dots & 0 & S_M^- \end{pmatrix} \tag{2.10}$$

but the representation and the dimension of the partitioned matrices, naturally, are different:

$$C_k^\pm = \begin{pmatrix} S_k^\pm \\ M_k^\pm \end{pmatrix}, \quad S_k^\pm = -iP_k M_k^\pm, \quad M_k^\pm = M_k E_k^\pm, \quad M_k = \|\mathbf{m}_1 \ \mathbf{m}_2 \ \dots \ \mathbf{m}_6\|$$

$$P_k = \|p_{ij}\|, \quad p_{ij} = C_{i3jn} \alpha_n, \quad i, j = 1, 2, 3$$

$$E_k^+ = \operatorname{diag}[1, 1, 1, e_k^{(1)}, e_k^{(2)}, e_k^{(3)}], \quad E_k^- = \operatorname{diag}[e_k^{(1)}, e_k^{(2)}, e_k^{(3)}, 1, 1, 1]$$

$$e_k^{(j)} = e^{-\sigma_j h_k}, \quad h_k = z_k - z_{k+1}$$

The blocks C_k^\pm and E_k^\pm have a dimension of 6×6 , while S_k^\pm and M_k^\pm have a dimension of 3×6 . The subscript k denotes that the corresponding matrices are expressed in terms of the characteristic numbers σ_j , the eigen column vectors \mathbf{m}_n and the elasticity constants C_{i3jn} for the k -th layer. When setting up the matrix A we used the matrix form of writing the Fourier symbols $\mathbf{U} = \mathcal{F}_{xy}[\mathbf{U}]$ and $\mathbf{T} = \mathcal{F}_{xy}[\boldsymbol{\tau}]$ of the strain and stress vector in each layer:

$$\mathbf{U}_k = M_k E_k(z) \mathbf{t}_k, \quad \mathbf{T}_k = -iP_k M_k E_k(z) \mathbf{t}_k$$

which followed from representation (2.8) and the relations of Hooke's law, where $E_k(z)$ is the diagonal matrix of the exponential functions, which occur in representation (2.8), and

$$E_k^+ = E_k(z_k), \quad E_k^- = E_k(z_{k+1})$$

For numerical stability of the solution of system (2.8), it is important that the exponential factors should not occur in the diagonal blocks of dimension 6×6 , formed from the last three and the first three columns of the matrices C_k^- and C_k^{+1} , and also in the diagonal blocks

of dimension 3×3 , consisting of the first three and the last three columns of the matrices S and S , respectively, while the exponential functions occurring in the remaining columns approach zero as $\alpha \rightarrow \infty$, i.e., the matrix A degenerates into a strictly partitioned-diagonal form.

This structure of the system matrix enables us to use iterational methods to solve it (for example, the Gauss–Seidel method), which is convenient for a large number of layers, when direct methods, which ignore the sparseness of A , become too difficult. Moreover, for large M we can use the recurrence relations

$$C_k^- \mathbf{t}_k = C_{k+1}^+ \mathbf{t}_{k+1}, \quad k = 1, 2, \dots, M - 1$$

and organize the solution in the form of a matrix double sweep, which requires only partitioned matrices of dimension 6, not containing the exponential factors $e_k^{(i)}$, to be inverted. For periodic laminated structures this inversion is carried out once, while for matrices raised to a higher power, which are obtained for a periodic cell, one can use well-known explicit representations.¹⁶

Since the vectors of the strains, due to concentrated loads $\mathbf{q} = \delta(x, y)\mathbf{i}_m$, applied along the coordinate unit vectors \mathbf{i}_m ($m = 1, 2, 3$), serve as the columns of the matrix K it is necessary to solve system (2.9) with three right-hand sides $\mathbf{f}_m = \{\mathbf{i}_m, 0, \dots, 0\}$ instead of $\mathbf{f} = \{\mathbf{Q}, 0, \dots, 0\}$.

The algorithm described enables us to obtain the values of $K(\alpha_1, \alpha_2, z, \omega)$ rapidly and stably for any type of anisotropy and number of layers. The strip ζ_n (the polar curves $\alpha = \zeta_n(\gamma)$) of the elements of the matrix K are found from the characteristic equation

$$\Delta(\alpha, \gamma, \omega) = \det A = 0 \tag{2.11}$$

Methods of searching for and calculating the residues, which occur in the representation for the excited waves (1.3), (1.4), on the whole remain the same as in the isotropic case.^{10,12}

3. Numerical examples

To check the reliability of the numerical results, in addition to standard test programs, which use the proposed approach (numerical satisfaction of the equations and boundary conditions), we compared our results with those of other authors. To do this we chose Refs 17 and 18, in which theoretical and experimental results for graphite–epoxy laminates with the following characteristics of the orthotropic layers (in the principal axes), are given

$C_{\alpha\beta}$	C_{11}	C_{12}	C_{13}	C_{22}	C_{23}	C_{33}	C_{44}	C_{55}	C_{66}	
A ($\rho = 1578 \text{ kg/m}^3$)	130.7	5.2	5.2	13.0	4.5	13.0	3.70	6.0	6.0	[17]
B ($\rho = 1550 \text{ kg/m}^3$)	110.7	7.5	7.5	14.1	7.3	14.1	3.37	6.1	6.1	[18]

The elasticity constants $C_{\alpha\beta}$ are given here in gigapascals ($1 \text{ GPa} = 10^9 \text{ N/m}^2$), and in the traditional abbreviated (matrix) numeration, in which the subscripts α and β correspond to the first and second pair of subscripts ij and kl of the component C_{ijkl} in accordance with the following rule

ij or kl	11	22	33	23	13	12
α or β	1	2	3	4	5	6

In the examples given below, the material A of thickness $H = 3 \text{ mm}$ (defined as the laminate AS4/3502, Ref. 17) is a packet of 24 layers, reinforced with graphite fibers, symmetrical about the middle plane $z = -H/2$. In each layer the fibers are parallel to the x_1, x_2 planes and between them. In the first six layers they are oriented at an angle of $+45^\circ$ with respect to the Ox_1 axis, and in the next six they are oriented at an angle of -45° . Further (for $z < -H/2$), in view of the symmetry, they are positioned in six layers with orientations of -45° and $+45^\circ$. The principal axes, with respect to which the elasticity constants $C_{\alpha\beta}$ are specified, are defined by the orientation of the fibers: the first of them coincides with the direction of the reinforcement and the third coincides with the Ox_3 axis. The packing of material B is similar, but in each set there are five rather than six layers (20 in all), with a common thickness $H = 2.72 \text{ mm}$.

Using mathematical model (2.1) - (2.4) the set of similarly oriented layers can be regarded as a single homogeneous layer, and hence both materials are modeled by a three-layer package with thicknesses of the outer layers $h_1 = h_3 = H/4$ and an inner layer $h_2 = H/2$. The values of the other moduli C_{ijkl} in the global system x are defined by the moduli C_{ijkl} , specified in the local system x' (i.e., by the values of $C_{\alpha\beta}$ given above) using the well-known transition formulae⁴

$$C_{ijkl} = p_{mi} p_{nj} p_{rk} p_{sl} C'_{mnr}$$

where p_{ij} are the components of the orthogonal rotation matrix $P: \mathbf{x} = P\mathbf{x}'$.

To carry out the calculations and to present the results, we used a dimensionless form, in which the thickness $H = 2.72 \times 10^{-3} \text{ m}$, the velocity of transverse waves $c = 4587 \text{ m/s}$ and the density $\rho = 1550 \text{ kg/m}^3$ were recorded as basis units of length, velocity and density. Here the dimensionless angular frequency $\omega = 2\pi Hf/c$, where f is the dimensional frequency in hertz.

Test comparisons for material A showed agreement of the frequency dependences of the strips $\zeta_n(\omega, \gamma)$ for a fixed angle $\gamma = 30^\circ$ (comparison with the data in Ref. 17, Fig. 3), and of the angular dependences $\omega/\zeta_n(\gamma)$ for a fixed frequency $\omega = 4$ for the symmetrical modes (Fig. 1a) and the antisymmetrical modes (Fig. 1b) (comparison with the data in Ref. 17, Fig. 5a and 5d respectively).

In polar coordinates (r, ϕ) the angular relations, shown in Fig. 1, are described by the equations $r = \omega/\zeta_n(\phi)$; in the isotropic case the strip ζ_n is independent of ϕ and the corresponding curves are circles. The values of ω/ζ_n agree with the values of the phase velocities of the waves, excited in an isotropic waveguide, and hence for anisotropic materials they can also be called phase velocities, but this only holds for plane waves, propagating in a fixed direction ϕ .¹⁷ For cylindrical waves, in accordance with asymptotic form (1.4), both the values of the phase velocities and the number of waves propagating from the source in the ϕ direction, are given by the relations $u_n(\phi) = \omega/s_n(\gamma_m)$ (Fig. 2).

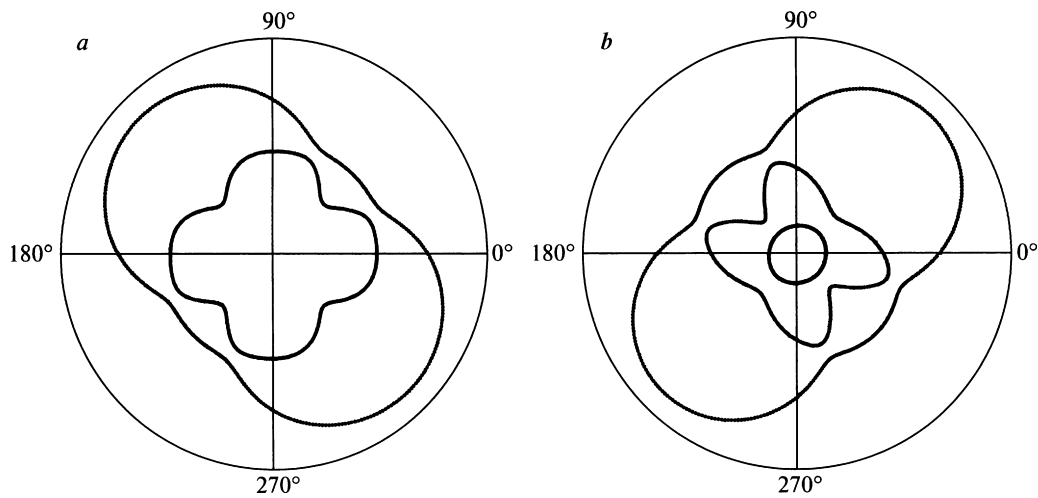


Fig. 1.

The asymptotic representation (1.3) and (1.4) enables us, without considerable computational cost, to analyse not only the spatial distribution of the amplitude of the wave field $\mathbf{u}(\mathbf{x})$, excited by a specified surface load \mathbf{q} , but also the transfer of wave energy, averaged over an oscillation period $T=2\pi/\omega$, described by the Poynting vector

$$\mathbf{e} = \{e_1, e_2, e_3\}, \quad e_k = -(\omega/2)\text{Im}(\mathbf{u}, \boldsymbol{\tau}_k)$$

where $\boldsymbol{\tau}_k$ is the vector of the stresses on an area with normal \mathbf{i}_k ($k=1, 2, 3$). Hence, as previously for isotropic waveguides,¹¹ it becomes possible to construct energy flow lines, which show the structure of the energy fluxes, to analyse the radiation patterns and the energy density distribution over the thickness of the material, and to investigate the frequency dependence of the total quantity of energy, entering from the source, its distribution between the excited waves, etc.

The anisotropy of the elastic properties has a considerable effect on the directivity of the outflow of energy from the region where the load is applied. Thus, for example, if an axisymmetric load $\mathbf{q}(r)$ acts on an isotropic waveguide, the radiated energy $|\mathbf{e}|$ is independent of the angle ϕ , while the energy flow lines are strictly along the radial rays, experimental measurements of the energy of surface waves, generated in material B by a vertical laser beam at a frequency $f=1$ MHz (Ref. 18, Fig. 6), show a pronounced concentration of the energy flux along the fibers of the upper layer ($\phi=45^\circ$) and in the orthogonal direction ($\phi=135^\circ$), coinciding with the orientation of the fibers in the inner layer. Calculations in the near zone, carried out using representations (1.2) and (1.3) for a concentrated vertical load $\mathbf{q}=\delta(\mathbf{x})\mathbf{i}_3$, showed, as previously,¹⁸ the nature of the distribution of the wave energy flux density, traveling from the source along the surface $z=0$. However, the energy flow lines, as one moves away from the source, deviating from the rectilinear radii, approach a direction parallel to the fibers of the upper layer (Fig. 3). Correspondingly, a large portion of the energy departs to infinity in the directions $\phi=45^\circ$ and $\phi=225^\circ$.

Whereas for measurements using a laser interferometer, only the surface waves are accessible, the directivity of the overall radiation of energy from the source at infinity obviously also depends on the flux density in the inner layers. Hence, to analyse the effect of the structure of the material on the outflow of energy, in addition to the radiation patterns of the surface waves we constructed diagrams for

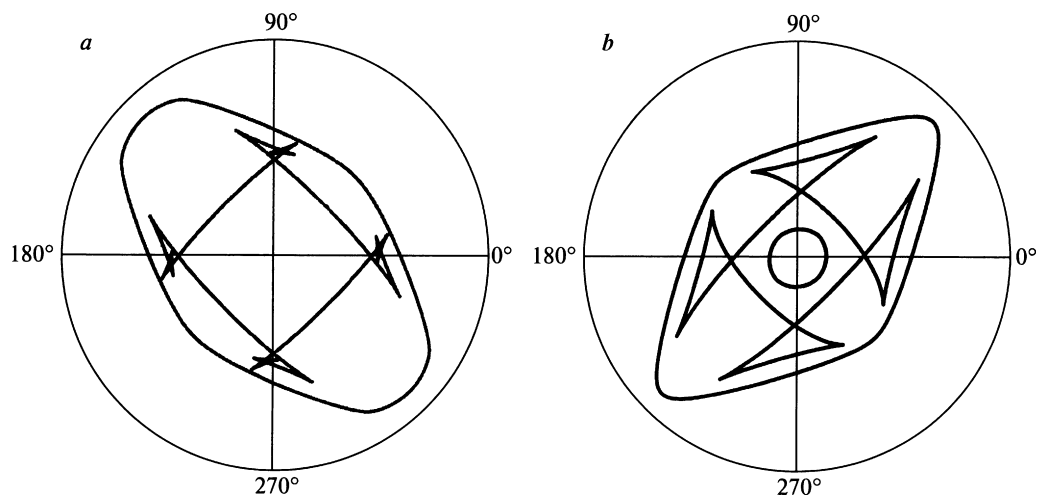


Fig. 2.

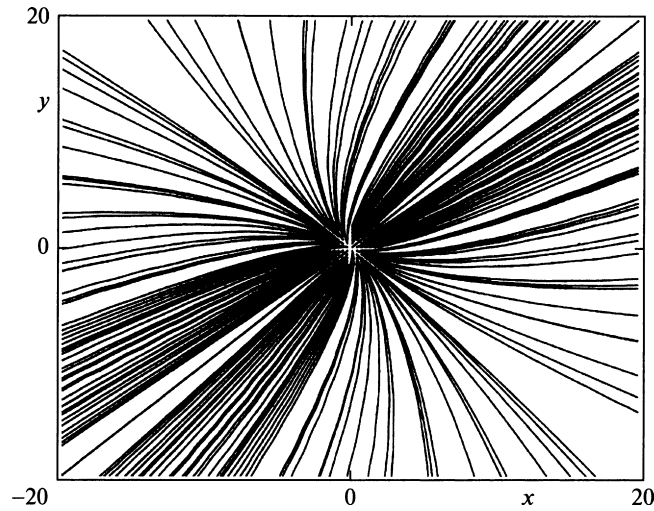


Fig. 3.

the total energy flux over the thickness, described by the function

$$E(\varphi) = \int_{-H}^0 |\mathbf{e}(r, \varphi, z)| r dz, \quad \kappa r \gg 1 \tag{3.1}$$

In Fig. 4 we show normalized diagrams of $E(\varphi)$, $0 \leq \varphi < 2\pi$ for material B when acted upon by a concentrated vertical load (Fig. 4a) and a shear circumferential load $\tau_{rz} = \delta(r - a)$ (Fig. 4b) at a frequency $f = 0.19$ MHz ($\omega = 0.71$). The circumferential source of radius $a = 5$ models the action of a circular piezoelectric plate, fixed to the surface of the composite material.⁶ Both loads are axisymmetric, but for the vertical load the energy is preferentially radiated along the fibers of the upper layer, while for a circular piezoelectric actuator it is radiated in equal measure along the fibers of both the outer and inner layers.

Once again we note that, in addition to the effect of the material structure, by means of the quantity $\mathbf{Q}(\alpha, \gamma)$ in solution (1.2) - (1.4) we also automatically take into account the characteristics of the source, whereas in the modal or ray analysis there is no source (natural solutions are constructed or the initial incident field is assumed to be specified). It is particularly important to take the source into account when its characteristics considerably influence the directivity of the radiation. For example, the action of a flexible rectangular piezoelectric cover with dimensions of $2a \times 2b$, attached to the surface $z = 0$, which is deformed due to the action of the electric current in the x direction, is usually modeled by a pair of concentrated shear stresses¹⁹

$$q_1(x, y) = \delta(x - a) - \delta(x + a), \quad |y| < b$$

$$Q_1(\alpha_1, \alpha_2) = 4i \sin \alpha_1 \sin b \alpha_2 / \alpha_2$$

In Fig. 5 we show the wave field $\text{Re}u_3(x, y, 0)$, excited by such a source in an isotropic plate (Fig. 5a) and in a plate made of material B (Fig. 5b) for $\omega = 1$, $a = 1$ and $b = 1$. By comparing them we can estimate the effect of the anisotropy of the properties of the material on the directivity of the radiation due to the source.

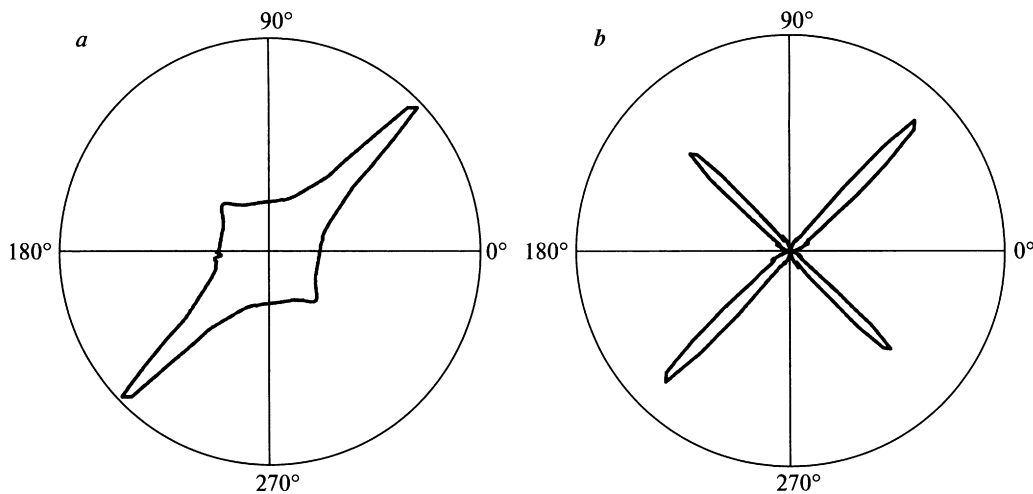


Fig. 4.

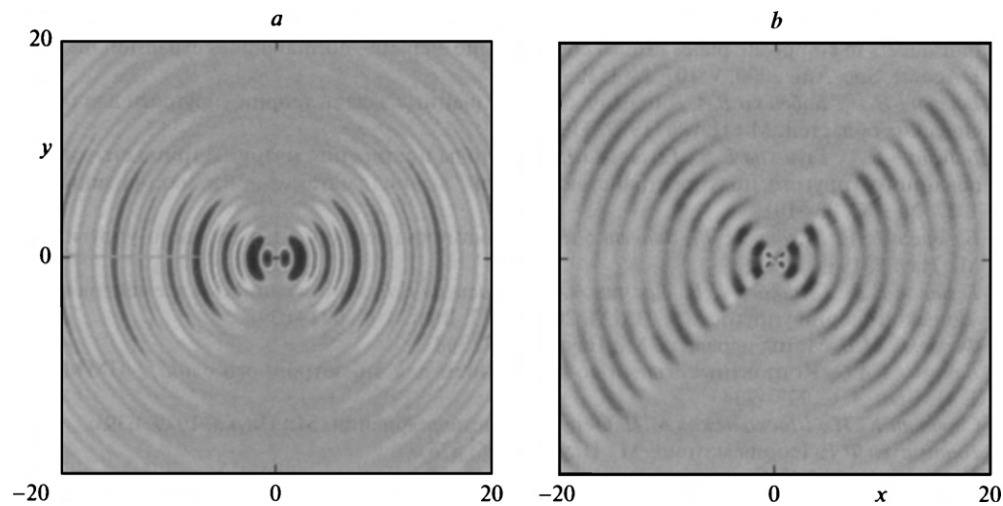


Fig. 5.

Acknowledgments

This research was supported by the Minobrnauka Analytic Departmental Special Purpose Programme (2.1.1/1231) and the Russian Foundation for Basic Research (07-01-00307).

References

1. Nayfeh AH. The general problem of elastic wave propagation in multilayered anisotropic media. *J Acoust Soc Am* 1991;**89**(4):1521–31.
2. Lowe MJS. Matrix techniques for modeling ultrasonic waves in multilayered anisotropic media. *IEEE Trans Ultrason Ferroelectr Freq Control* 1995;**42**(4):525–42.
3. Brekhovskikh LM, Godin OA. *The Acoustics of Laminated Media*. Moscow: Nauka; 1989.
4. Lekhnitskii SG. *Theory of Elasticity of Anisotropic Elastic Body*. San Francisco: Holden-Day; 1963.
5. Christensen RM. *Mechanics of Composite Materials*. New York: Wiley; 1979.
6. Raghavan A, Cesnik CES. Review of guided-wave structural health monitoring. *The Shock and Vibration Digest* 2007;**39**(2):91–114.
7. Su Zh, Ye Lin, Lu Ye. Guided Lamb waves for identification of damage in composite structures: A review. *J Sound and Vibration* 2006;**295**(3–5):753–80.
8. Moulin E, Assad J, Delebarre Ch, Osmont D. Modeling of Lamb waves generated by integrated transducers in composite plates using a coupled finite element–normal modes expansion method. *J Acoust Soc Am* 2000;**107**(1):87–94.
9. Vorovich II, Babeshko VA. *Dynamic Mixed Problems of Elasticity Theory for Non-classical Regions*. Moscow: Nauka; 1979.
10. Babeshko VA, Glushkov YeV, Glushkova NV. Methods of constructing Green's matrix of a stratified elastic half-space. *Zh Vychisl Mat Mat Fiz* 1987;**27**(1):93–100.
11. Babeshko VA, Glushkov YeV, Zinchenko ZhF. *The Dynamics of Inhomogeneous Linearly Elastic Media*. Moscow: Nauka; 1989.
12. Glushkov YeV, Glushkova NV, Yeremin AA, Mikhas'kiv VV. The layered element method in the dynamic theory of elasticity. *Prikl Mat Mekh* 2009;**73**(4):622–34.
13. Fedoryuk MV. *The Method of Steepest Descents*. Moscow: Nauka; 1977.
14. Vatul'yan AO. Contact problems with adhesion for an anisotropic layer. *Prikl Mat Mekh* 1977;**41**(4):727–34.
15. Sirotnin Yul, Shaskal'skaya MP. *Principles of Crystal Physics*. Moscow: Nauka; 1979.
16. Gantmacher FR. *The Theory of Matrices*. New York: Chelsea; 1974.
17. Wang L, Yuan FG. Group velocity and characteristic wave curves of Lamb waves in composites: Modeling and experiments. *Compos Sci and Technol* 2007;**67**(8):1370–84.
18. Balasubramaniam K, Krishnamurthy CV. Ultrasonic guided wave energy behaviour in laminated anisotropic plates. *J Sound and Vibrat* 2006;**296**(4–5):968–78.
19. Giurgiutiu V. Lamb wave generation with piezoelectric wafer active sensors for structural health monitoring. Proc. SPIE. 2003. Paper No. 5056-17.

Translated by R.C.G.